TDMA-based scheduling for multi-hop wireless sensor networks with 3-egress gateway linear topology

doi: https://doi.org/10.1016/j.iot.2021.100398

TDMA-based scheduling for multi-hop wireless sensor networks with 3-egress gateway linear topology

ARTICLE INFO

Keywords:
Multi-hop wireless sensor networks
TDMA-based transmission scheduling
Linear topology
Lagrangian multiplier method

ABSTRACT

We have studied packet transmission scheduling on multi-hop wireless sensor networks with 3-egress gateway linear topology, called Y-shaped topology. In every one cycle period, each node generates and forwards data packets that are bounded for either of the gateways at edges. In this paper, we focus on centrally-managed Time Division Multiple Access (TDMA)-based slot allocations and design a packet transmission scheduling framework combining with the basic redundant transmission to reduce and recover packet losses. On each of three types of path models to cover all possible routing on Y-shaped topology, we efficiently derive a global static time-slot allocation. The derived time-slot allocation exactly maximizes the probability that all packets are successfully delivered to one of the gateways within one cycle period, which cannot be achieved by existing scheduling schemes.

1. Introduction

Nowaydays, multi-hop wireless networks are in widespread use because of their cost-efficiency and flexibility in deployment and operation. They can connect nodes in an extensive coverage area larger than a single hop radio range with proper transmission power. Consequently, multi-hop wireless networks are an excellent candidate for emerging IoT systems when a commercial communications infrastructure is unavailable or costly. However, especially when the number of hops is large, multi-hop wireless networks for field monitoring often suffer from frequent packet losses due to attenuation and fading on each link as well as radio interferences of simultaneous transmissions among nodes. Furthermore, in typical multi-hop sensor network scenarios, since each packet conveying sensing data should be forwarded toward one of the sink nodes, the links near a sink are likely congested to forward all packets coming from upstream nodes. In general, to cope with frequent packet losses, researchers have proposed proactive approaches, e.g., redundant transmissions of original or coded packets with forwarding erasure correction (FEC); reactive approaches, e.g., retransmission of lost packets by automatic repeat request (ARQ); and combinations of them, e.g., Hybrid ARQ. To avoid or reduce interferences (conflicts) of simultaneous packet transmissions, researchers have also proposed centralized scheduling-based approaches, e.g., time division multiple access (TDMA), and decentralized contention-based approaches, e.g., carrier-sense multiple access with collision avoidance (CSMA/CA).

This study targets a stationary but lossy backbone network to forward the sensing data from sensors to the multiple egress "gateways" that are connected to a central data collection via an infrastructural reliable network. Therefore, a "node" does not represent each sensor but rather a low-cost relay node. Each node periodically gathers sensing data from nearby end sensors and forwards them in a hop-by-hop store-and-forward manner to one of the gateways within one cycle time-period. The neighboring relay nodes communicate with each other by a simple omnidirectional antenna using the same single frequency. There are some ways to gather the sensing data from end sensors connected to the relay node, e.g., a short-range wireless link different from the links between relay nodes in terms of types and frequencies, but it is out of the paper scope.

In this study scope, to be more exact, we consider kinds of stationary "linear topology". They are more simple than mesh, complex, or dynamic topologies, but typical for geographically elongated field monitoring in which surveillance sensors are deployed along with a roads, rivers, or electricity pylons networks. In addition, since targeting a dedicated network consisting of low-cost relay nodes, gateways, and a central server, we adopt a centrally-managed TDMA-based packet transmission scheduling with redundant transmissions assuming that the link layer does not provide any ARQ and transmission power adaptation mechanisms. In linear topologies, the number of neighboring nodes is limited, and the distance between of neighboring nodes is long [1]. Therefore, the number of potential interference patterns and possible routing options are also limited, which may allow us to pursue the optimality easier compared with general dense topologies. On the other hand, the small number of possible routes will be a disadvantage in terms of robustness

ORCID(s):

against a failure of nodes or links. It is worth noting that we focus on cases in which multiple gateways as the sinks are placed outer-side rather than inner-side of a linear topology, which is essentially different from "tree topologies". If a gateway is placed in a central area, there are "interferences at the head" among the different flows of packets. Tree topologies are often used in reducing the number of necessary gateways but may suffer from heavy congestions around gateways due to the interferences at the head. In our previous work, we have focused on tandemly-arranged topology networks with two gateways at both edges of a linear network [2, 3, 4]. In that the topology, data transmission rate (i.e., bandwidth), each link's time-averaged packet loss rate, the packet size, and each node's packet generation rate are known, we have successfully derived an "optimal" static packet transmission time-slot allocation under a basic redundant transmission scheme.

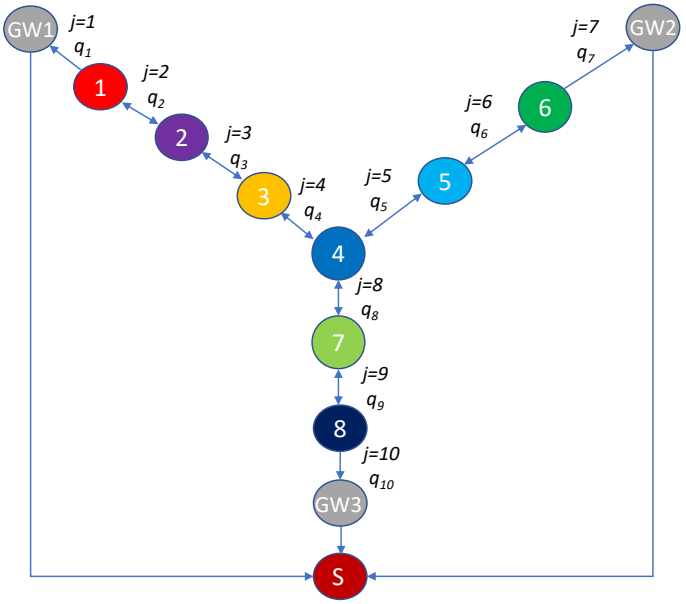

Figure 1: An example of Y-shaped network topology used in this research

In this paper, we present the models and the performance investigation on the 3-egress gateway linear topology that is a linear topology with three gateways at the edges, called Y-shaped topology illustrated in Fig. 1. In any Y-shaped topology, there is a central node that potentially has three links but some of the three links are not necessarily used for data transmission. Our proposed scheme aims at a global static time-slot allocation on Y-shaped topology to maximize the theoretical probability that all packets are successfully delivered to one of the gateways with redundant transmissions within one cycle period. In contrast to tandemly-arranged linear topologies with two gateways at the edges, there are "interferences at the tail" among the different flows of packets. However, such interferences can be efficiently avoidable because the data forwarding directions are opposite, in contrast to tree-like topologies with a gateway at center. This paper is a fully-extended version of our most recent publication, in which we used the term T-shaped topology [5]. The extension includes complete modeling representing all possible variations of this topology, a design framework of optimal scheduling that covers all models, its detailed derivations, and an investigation on performance with diverse cases. Note that, in our scheme, a central management server is assumed to know or estimate necessary information such as the packet loss rate of each link, compute a global time-slot allocation, and deliver the derived schedule to each node. Such system implementation issues will be discussed later in the Section 6, as it is not the main scope of this paper.

The rest of this paper is organized as follows. The related work is reviewed in Section 2. Y-shaped topology and the path models are defined in Section 3. Section 4 explains how to derive optimal time-slot allocations using an example topology, which is evaluated through numerical simulations in Section 5. Discussions are provided in Section 6 and finally, Section 7 concludes the paper. The appendix is given to explain an example of the detailed derivation of the mathematical formula.

2. Related work

For multi-hop wireless networks, there have been a variety of studies devoted to coping with the lossy unreliable wireless radio links and the conflicts (interferences) among simultaneous transmissions on adjacent links depending on a variety of requirements and restrictions. Even in TDMA-based transmission scheduling to resolve two fundamental bottlenecks of multi-hop wireless networks, various methods have been developed [6]. They have been classified into TDMA node scheduling, TDMA link scheduling, TDMA cross-layer scheduling, and hybrid TDMA algorithms, based on the difference in network topology, node degree, and type of node. Among them, TDMA node scheduling and TDMA link scheduling have been considered as a well-known solution due to their simple and popular models in wireless sensor networks. Therefore, we will focus on these approaches and their achievements via some recent publications in this section. In theory, the algorithms are conducted by defining a conflict-free TDMA for a given set of links, which is formulated as a graph coloring. In addition, wireless conflicts are able to model with conflict graphs [7], [8]. As a result, for example, [7] obtained a graph coloring on the conflict graph, a conflict-free schedule formed from independent sets with appropriate cardinality. [9] addressed a collision in two conflicting adjacent links by utilizing a novel distributed randomized time slot scheduling algorithm, called distributed implementation of RAND (DRAND). It was expected to resolve an assigning different time slots problem in practice based on the assumption that clock drifts among nodes are finitely bounded although their drift rates because it is a simple method with the potential to practical application. In their TDMA slot assignment issue, they concentrated on maximize slot numbers by using heuristic solutions for a coloring assignment algorithm. Besides, they also considered about other two quantities, including running time, and message complexity, which have a significant influence on the overall performance of their proposed method. Sharing the similar consideration about coloring graph [9], [10] introduced three algorithms, consisting of node-based scheduling, level-based scheduling, and distributed scheduling algorithms to determine the small length conflict-free assignment of slots for efficient solving scheduling problem. The node-based and level-based scheduling algorithms were constructed based on the conflict graph (GC), which corresponded to the tree graph G and interference graph C. They included two sections, coloring and scheduling. For the first task, the heuristic coloring algorithm was employed to assign the smallest color to the nodes in the condition that none of the nodes of the same color have an edge in the conflict graph. In terms of scheduling, these algorithms were built by allocating slots to each node to ensure that all packets reach the gateway. The difference between these methods was mainly attributed to the requirement for topology information. However, this request may not be satisfied in the large network. Hence, the third method, distributed algorithms, was generated to tackle this issue and maintain the scalability in the system. In practice, the distributed algorithms scheduled the nodes based on the local topology information of the nodes. [11] introduced another approach to generate the short schedule in the tree network topology and solve the scheduling problem for TDMA. It was conducted through the min-max and min-sum models, which their performance was greatly affected by CPU time. Numerical examples determined that the short schedule built in their method only achieved, at the expense of the CPU time. In specific, a min-max model provided the optimal schedule overcoming the constraints, but it required unrealistic CPU time. In contrast, a min-sum model only satisfied the requirement relating to short CPU time but could not guarantee the overall performance in practice. Hence, they targeted the heuristics as an coorperated components to their existing models to enhance the practical possibility. [12] utilized a scheduling algorithm, which was developed from the collaboration of nodes, including three phases REQ, REPLY, and ACK, to improve the packet receive ratio and energy efficiency. The proposed method in this work was a collaboration-based distributed strategy for the TDMA scheduling algorithm to transmit all data to sink in an interference-aware way. There were two parts in this algorithm, network initialization, and schedule transmission, which were constructed to establish the schedule of the node and collect data following it. In comparison with the equivalent models, the better reliability in packet delivery and energy efficiency brings up the higher possibility to employ it in systems, which require energy sensitivity and guarantee for high data gathering. [13] represented an other approach to address scheduling problems based on a computational method using quantum annealing in a tree and medium access control network topology. In detail, they attempted to solve maximum independent set problems with weights of vertices repeatedly. Results obtained revealed that the computation time in this method was less than its equipvalent studies, which excluded NetworkX, a Python package for the study of complex networks, and relatively equal to works based on NetworkX. [14] Introduced different solution for scheduling problem by the centralized approach. This work utilized a TDMA-based wireless sensor network where a large networks, where the sink manages up to hundred nodes streaming data transmitted to a sink through a tree topology. Therefore, they developed two algorithrms, Joint Scheduling and Routing Algorithms—JSRA1 and JSRA2, providing different throughput-delay compromises. These methods were expected to jointly resolve routing (Tree

Formation), radio resource assignment (Scheduling) and power control (Power Selection). [15] dealt with TDMA-based wireless mesh networks with multiple gateway nodes and proposed a spanning tree construction algorithm to maximize the traffic volume transferred between the mesh network and the central server via gateways. As a result, the interference-aware tree construction (LITC) algorithm built up following this approach was increase the overall performance of system up to 3.1 times and significantly reduce the time complexity. [16] addressed the guarantee issues of distributed scheduling in wireless networks by a simple distributed scheduling strategy. They proved the guarantees of performance for maximal scheduling under arbitrary interference models and topologies. Besides, it was determined to maintain a constant fraction of the maximum throughput region, which was possible to generalize to other multicast communication and ensure the fairness of rate allocation.

However, almost all of these studies concentrated on developing conflict graphs or heuristics to avoid interference of simultaneous data transmission on general network topology, and they do not deal with optimal redundant transmissions to recover lost packets. On the other hand, our previous work [2, 3, 4] in this theme provided a packet transmission scheduling framework restricted to tandemly-connected topologies only.

In comparison with previous studies sharing interest in TDMA-based scheduling, regardless of a targeting performance metric, both routing in space and scheduling in time should be jointly designed in general. As a strong advantage of Y-shaped topology, the routing (we call it the path model) can be decided based solely on a pair of separation links. Although the number of such pairs is increased as the number n of links increased (in the order of n^2 at worst), the number of prospective candidates can be very limited in a branch and bound manner. Then, we classify the path models into three general types and propose the method to design a schedule (a static slot allocation) that is optimal in terms of our targeting performance metric. For each path model, there may be a few patterns of prospective interference-free slot allocation in terms of our targeting performance metric. The number of such patterns to consider is also limited due to the future of linear topologies with the gateways at the edges. Finally, for each allocation pattern, we need to solve a constraint maximization problem to decide how many consecutive slots should be allocated to each packet on each link for redundant transmissions in a given slot allocation pattern. As a strong advantage of our proposed approach, by applying Lagrange multiplier method, we can get the solution based solely on solving a few non-linear equations with a single real-number variable for each, which can be solved very efficiently by a numerical solver (Matlab in our case). In short, the contribution of this paper is as follows.

- The Y-shaped topology (with three gateways at the edges) is modeled that is useful as a backbone of mutihop wireless sensor networks for field monitoring while so simple to allow us to avoid an combinatorial explosion problem.
- A general framework on Y-shaped topology to find a static interference-free allocation of time-slots is proposed to maximize the probability that all packets are successfully delivered through lossy links to one of the gateways with redundant transmissions within a given one cycle period, which is explained on a 8-node example topology.
- On that example topology, an exact solution is shown to be efficiently obtained by considering prospective slot allocation patterns and also by applying Lagrange multiplier method to solve a relaxed version of the constrain maximization problem, which performance is investigated in detail with diverse cases of packet loss rate setting.

On the other hand, the limitation remains as follows; discussed later in Section 6.

- The framework and the solutions are explained only in cases that the packet generation rates of nodes and the data transmission rates of links are homogeneous, while applicable to heterogeneous cases in principle.
- Only a basic redundant transmissions is considered in which a node just redundantly transmits each of its possessed packets in a specific times according to the given time-slot allocation, while an inter-packet coding is beneficial to the success delivery probability.
- Only a centrally-managed logical framework is provided. The system architecture and implementation issues to realize the logical framework of wireless sensor networks should be discussed.

3. Y-shaped topology model

In Y-shaped network topology, the nodes and links are numbered separately (starting from 1) as shown in Fig. 1. The packet loss rate of link j is denoted as q_j ($0 < q_j < 1$), and the packet generation rate of node i is denoted as

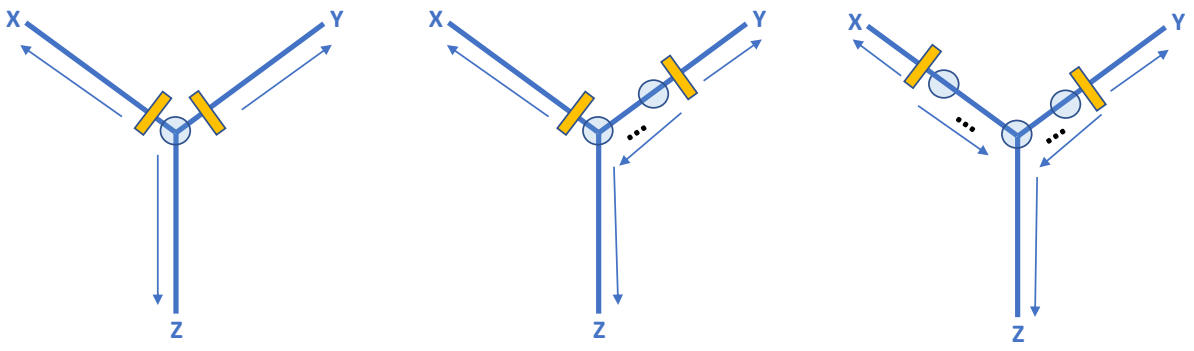

Figure 2: Y-shaped network topology model

positive integer r_i. As explained in Section 1, each node considered here is a relay node of the Y-shaped backbone of a sensor network. Hence the packet generation rate of a node represents the number of packets to convey the total amount of sensing data in one cycle period of D gathered from the end sensors managed by the node. In other words, node i is assumed to generate r_i packets at the beginning or before of each D, and those packets are forwarded toward a gateway X, Y, or Z. For concise formulations, all packets are assumed to have the same size and all links are to have the same data transmission rate. Therefore, let U be the time duration of one time-slot, i.e., one packet can be transmitted on a link between adjacent two nodes in U unit time, Then the total number T of slots in one cycle period is equal to D/U.

We assume that each packet is forwarded along a single path (not a multi-path) toward only one of the three gateways. Based on this assumption, this study models Y-shaped topology in three types as shown in Fig. 2. A separation link is a link on which no packet is transmitted because the two nodes at both sides of the link send packets in opposite directions, i.e., the link is between two nodes each of which is at the most upstream of a path. Since Y-shaped topology has a single central node and three branches (called "segment") terminated by gateways X, Y, and Z there should be two separation links that separate the topology into three paths with different numbers of nodes in general. We call it "the path model" representing packet routing paths; different path models can be considered by choosing the locations of the separation links. To be more exact, we can assume one separation link is in the segment of X and the other is in the segment of Y; no separation link in the segment of Z without loss of generality. In this sense, the gateway name X, Y, and Z should be given depending on the path model. Depending on the locations of separation links, all nodes are grouped into three groups called S_X, S_Y, and S_Z which are the set of nodes whose packets are forwarded to X, Y, and Z, respectively. It is called the l-r-d model where l, r, and d represent the number of nodes in S_X, S_Y, and S_Z, respectively. To avoid an uncertainness, we can assume $l \geq r$ without loss of generality by assigning the name X and Y appropriately. Furthermore, based on the locations of separation links, three types of path models are considered. Type 1: no node on segment of X and Y is in S_Z. Type 2: some nodes on only one of segments of X and Y are in S_Z. Type 3: some nodes on segment of X and also some nodes in segment of Y are in S_Z.

The three types would represent all possible variations of Y-shaped network topologies, affecting the potential interference patterns among nodes nearby the central node that strongly impact the design of slot allocations, i.e., slot allocation patterns. For example, as shown in Fig. 3, if the first separation link is set between nodes 3 and 4, and the second is set between nodes 4 and 5, then the path model is the 3-2-3 model and this is Type 1. Group S_X has 3 nodes in where the packets are forwarded to gateway X ($S_X = \{1, 2, 3\}$), group $S_Y = \{5, 6\}$, and group $S_Z = \{4, 7, 8\}$. Similarly, Fig. 6 and Fig. 8 illustrate the 2-2-4 model of Type 2 and 2-1-5 model of Type 3, respectively.

On the time-slot allocation to avoid interferences by simultaneous transmissions by different nodes in a network, Y-shaped topology in our targeting scenarios have a notable advantage. Since the egress gateways are located at the edges of each segment and all packets in a group (S_X, S_Y, or S_Z) are forwarded towards its gateway (X, Y, or Z), potential interferences among different groups happen only at nodes near the central node, i.e., interferences at the tail, and thus can only be in the initial phase of one cycle period. Therefore, except for a small number of those interference patterns, we only consider interferences among successive nodes in the same group. Consequently, the prospective patterns of slot allocation are significantly limited compared with tree-based topologies where the egress gateways are

at center and more general mesh-like topologies.

4. Path models and time-slot allocation

In designing a global static time-slot allocation, there are two issues: how much each node can utilize a limited number T of time-slots with redundant packet transmissions by considering the upstream-downstream relationship among nodes and the packet loss rate of each link; and how much it can avoid radio interferences in simultaneous transmissions. To solve those issues, the following steps are performed. First, we list all possible path models on a given Y-shaped topology. Second, for each path model, by considering the potential interference to avoid around the central node, we list all prospective candidates of "slot allocation patterns". To prohibit nearby nodes from harmful simultaneous transmissions, a static interference avoidance policy is necessary. Note that, although the number of prospective candidate patterns is limited in Y-shaped topology as noted in Section 3, we need to use geographical information such as distances and environmental conditions in general, which are not represented by an abstract topology. In this paper, we adopt a simple hop distance-based policy for interference avoidance to show the example concisely, while more a complicated policy is applicable as long as it is static. For each pattern of each path model, we derive a static time-slot allocation to maximize the theoretical probability that all packets are successfully delivered to gateways through lossy links within the total time-slots of T using redundant packet transmissions against packet losses. Lastly, by comparing all results in terms of the theoretical probability of successful delivery, we can select the best path model with the best slot allocation.

We explain an optimal static time-slot allocation for each allocation pattern of each path model on an example topology with 8 nodes illustrated in Fig. 1. To express a slot allocation, in general, we denote $s_{i,j,k}$ as the number of slots allocated, i.e., available to use, for the k-th packet generated by node i on link j in each cycle period. In other words, each node redundantly transmits a possessed packet (which is originally the k-th packet generated by node i) on downstream link j in $s_{i,j,k}$ times. However, for concise explanation, packet generation rate r_i is assumed to be 1 and thus $s_{i,j}$ is used instead of $s_{i,j,k}$. The extension to heterogeneous packet generation rates $\{r_i\}$ is somewhat straightforward as shown in Appendix A. Furthermore we introduce $s'_{i,j}$ to indicate the number of slots for an early stage transmission which happens before or at the same time of transmission of the most upstream node in the path, i.e., a concurrent use of the same time-slots for the same direction transmissions to increase the efficiency. We also note that, when a packet is lost and not recovered on some link (i.e., retransmissions of the packet on the link fail at all), the slots originally allocated to that lost packet are used for the next packet on each downstream link.

In general, the maximization problem for optimal slot allocations is defined as follows. The success probability of delivering a packet generated by node i is denoted by $M_i(\mathsf{s_i})$ that can be calculated based on a slot allocation $\mathsf{s_i} = \{s_{i,j}, s'_{i,j} | j = 1, \ldots, 10\}$ for $i = 1, 2, \ldots, 8$. Hence the problem to solve is

$$
\begin{aligned}
\max\ M(\mathsf{s}) &= \prod_{i=1}^{8} M_i(\mathsf{s_i}) \ \text{ subject to} \\
T &= \text{(a linear function of } \mathsf{s} \text{ in group X)} \\
T &= \text{(a linear function of } \mathsf{s} \text{ in group Y)} \\
T &= \text{(a linear function of } \mathsf{s} \text{ in group Z)}
\end{aligned}
$$

where $\mathsf{s} = \{s_{i,j}, s'_{i,j} | i = 1, 2, \ldots, 8;\ j = \ldots\}$.

The M is the theoretical probability that all packets are successfully delivered to gateways if each packet is lost randomly and independently of other packets. Furthermore, maximizing M is equivalent to maximizing the log-sum of M_i, i.e., $\sum_{i=1}^{8} \log M_i(\mathsf{s_i})$, which generally intends a fair balance among the nodes in terms of the success probability of delivering a packet generated by each node.

4.1. Static slot allocation for the 3-2-3 model

Fig. 3 shows the 3-2-3 path model. In this example, since we assume nodes 3 and 7 are in the radio propagation distance, 3 and 4 cannot send at the same time to avoid interference at node 7. Since nodes 5 and 7 are in the propagation distance, 5 and 4 cannot send at the same time to avoid interference at node 7. On the other hand 3, 5, and 7 can send to their next node at the same time. We have two patterns for slot allocations. In Pattern 1, we prioritize the transmission

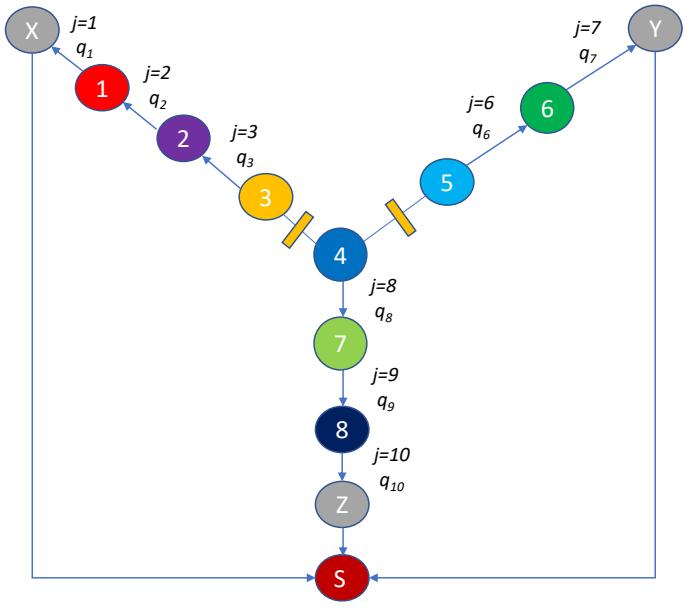

Figure 3: The 3-2-3 path model in the network topology

in groups S_X (node 3-2-1) and S_Y (node 5-6) first, then group S_Z (node 4-7-8). In Pattern 2, we prioritize the group S_Z first, then groups S_X and S_Y. In other words, in Pattern 2, the most upstream side node toward Z (i.e., node 4) can start its transmission earlier than the most upstream nodes toward X and Y (i.e., nodes 3 and 5).

Pattern 1 as illustrated in Fig. 4 is adopted when node group S_X or S_Y is a bottleneck. We solve a sub-problem for group S_X and S_Y first. In group S_X,

$$\begin{aligned} M_1 &= (1-q_1^{s_{1,1}}), \\ M_2 &= (1-q_1^{s_{2,1}})(1-q_2^{s_{2,2}}) \\ M_3 &= (1-q_1^{s_{3,1}})(1-q_2^{s_{3,2}})(1-q_3^{s_{3,3}}) \end{aligned} \tag{1}$$

In group S_Y,

$$M_5 = (1-q_6^{s_{5,6}})(1-q_7^{s_{5,7}})$$

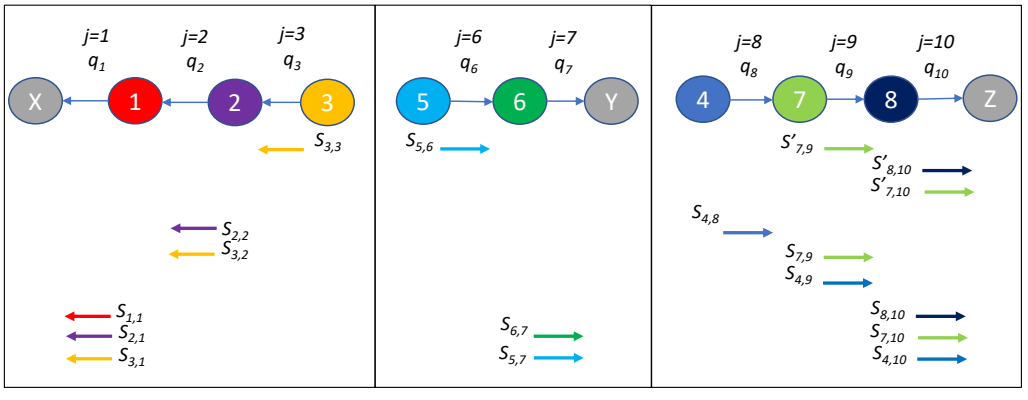

Figure 4: Transmission scheduling on 3-2-3 model (Pattern 1, all r_i=1)

$$M_6 = (1 - q_7^{s_{6,7}}) \tag{2}$$

In group S_Z, $s_{7,9}$ and $s'_{7,10}$ cannot be 0 at the same time, in any optimal schedule.

$$\begin{aligned} M_8 &= (1 - q_{10}^{s_{8,10}+s'_{8,10}}), \\ M_7 &= \begin{cases} (1 - q_{10}^{s'_{7,10}+s_{7,10}})(1 - q_9^{s'_{7,9}}) & \text{if} \quad s_{7,9} = 0, \\ (1 - q_{10}^{s_{7,10}})(1 - q_9^{s'_{7,9}+s_{7,9}}) & \text{if} \quad s'_{7,10} = 0, \end{cases} \\ M_4 &= (1 - q_{10}^{s_{4,10}})(1 - q_9^{s_{4,9}})(1 - q_8^{s_{4,8}}) \end{aligned} \tag{3}$$

First, to get a slot allocation in group S_X that maximizes $M_1 M_2 M_3$ subject to

$$T = s_{1,1} + s_{2,1} + s_{2,2} + s_{3,1} + s_{3,2} + s_{3,3}, \tag{4}$$

we apply the Lagrangian multiplier to a relaxation version of this problem to derive equations Eq. (5) where $s_{i,j}$ are not restricted to natural numbers and α is an unknown adjunct variable; (see Appendix A).

$$\begin{aligned} s_{1,1} = s_{2,1} = s_{3,1} = -\frac{\log(1 - \alpha \log(q_1))}{\log(q_1)} \\ s_{2,2} = s_{3,2} = -\frac{\log(1 - \alpha \log(q_2))}{\log(q_2)}, \quad s_{3,3} = -\frac{\log(1 - \alpha \log(q_3))}{\log(q_3)} \end{aligned} \tag{5}$$

From Eqs.(4) and (5), α can be numerically solved to get the real number solution $\{s_{i,j}\}$ of the relaxed problem. Then we should seek an appropriate natural number solution as the number of allocated slots near the derived real number solution. Let $\{s^*_{i,j}\}$ be the natural number solution obtained for S_X; let $\mathbf{a_3}$ be $s^*_{3,3}$.

Next, independently and similarly to S_X, to get a slot allocation in group S_Y that maximizes $M_5 M_6$ subject to

$$T = s_{5,6} + s_{5,7} + s_{6,7}, \tag{6}$$

we have

$$s_{5,7} = s_{6,7} = -\frac{\log(1 - \beta \log(q_7))}{\log(q_7)}, \quad s_{5,6} = -\frac{\log(1 - \beta \log(q_6))}{\log(q_6)} \tag{7}$$

where β is an unknown adjunct variable. From Eqs.(6) and (7), β can be numerically solved to get the real number solution $\{s_{i,j}\}$ of the relaxed problem. Then we obtain the natural number solution $\{s^*_{i,j}\}$ for S_Y. Let $\mathbf{a_6}$ be $s^*_{5,6}$.

Finally, to find a slot allocation in group S_Z using $\mathbf{a} = \max(\mathbf{a_3}, \mathbf{a_6})$, we tentatively maximize $M_4 M_7 M_8$ without considering $s'_{8,10}$, $s'_{7,10}$, $s'_{7,9}$ subject to

$$T = s_{8,10} + s_{7,9} + s_{7,10} + s_{4,8} + s_{4,9} + s_{4,10} \tag{8}$$

where its solution $\{s^*_{i,j}\}$ can be solved in the same way. Let $\mathbf{b}_8$ be $s^*_{4,8}$, $\mathbf{b}_9$ be $s^*_{4,9}$, $\mathbf{b}_{10}$ be $s^*_{4,10}$. There are five cases by considering interference avoidance in S_Z with $s^*_{3,3}$ slots in S_X and $s^*_{5,6}$ slots in S_Y: (c1) $\mathbf{b}_9 \geq \mathbf{a}$; (c2) $\mathbf{b}_9 < \mathbf{a}$ and $\mathbf{b}_{10} \geq \mathbf{a}$; (c3) $\mathbf{b}_9 + \mathbf{b}_{10} \geq \mathbf{a}$; (c4) $\mathbf{b}_9 + 2\mathbf{b}_{10} \geq \mathbf{a}$; (c5) $\mathbf{b}_9 + 2\mathbf{b}_{10} < \mathbf{a}$.

- In (c1), a final natural number solution is:

$$\begin{aligned} s_{4,8} = \mathbf{b}_8, \quad s'_{7,9} = \mathbf{a}, \quad s_{7,9} = \mathbf{b}_9 - \mathbf{a}, \quad s_{4,9} = \mathbf{b}_9 \\ s_{8,10} = s_{7,10} = s_{4,10} = \mathbf{b}_{10}, \quad s'_{8,10} = s'_{7,10} = 0 \end{aligned}$$

- In (c2), a final natural number solution is:

$$\begin{aligned} s_{4,8} = \mathbf{b}_8, \quad s'_{7,9} = 0, \quad s_{7,9} = s_{4,9} = \mathbf{b}_9, \\ s_{8,10} = \mathbf{b}_{10} - \mathbf{a}, \quad s_{7,10} = s_{4,10} = \mathbf{b}_{10}, \quad s'_{8,10} = \mathbf{a}, \quad s'_{7,10} = 0 \end{aligned}$$

- In (c3), a final natural number solution is:

$$s_{4,8} = \mathbf{b}_8, \quad s'_{7,9} = \mathbf{b}_9, \quad s_{7,9} = 0, s_{4,9} = \mathbf{b}_9, \quad s'_{8,10} = \mathbf{a} - \mathbf{b}_9,$$
$$s_{8,10} = \mathbf{b}_{10} - (\mathbf{a} - \mathbf{b}_9), \quad s_{7,10} = s_{4,10} = \mathbf{b}_{10}, \quad s'_{7,10} = 0$$

- In (c4), a final natural number solution is:

$$s_{4,8} = \mathbf{b}_8, \quad s'_{7,9} = \mathbf{b}_9, \quad s_{7,9} = 0, \quad s_{4,9} = \mathbf{b}_9, \quad s'_{8,10} = \mathbf{b}_{10}, \quad s_{8,10} = 0,$$
$$s'_{7,10} = \mathbf{a} - (\mathbf{b}_{10} + \mathbf{b}_9), \quad s_{4,10} = \mathbf{b}_{10}, \quad s_{7,10} = \mathbf{b}_{10} - (\mathbf{a} - (\mathbf{b}_{10} + \mathbf{b}_9))$$

- Case (c5) requires to solve other two equations independently:

  (i) For nodes 7 and 8, the time-slot region length is $\mathbf{a}$.

$$\mathbf{a} = s_{7,9} + s_{7,10} + s_{8,10}$$

  By letting $s^*_{i,j}$ be its solution, a final natural number solution is:

$$s'_{7,9} = s^*_{7,9}, \quad s_{7,9} = 0, \quad s'_{7,10} = s_{7,10} = s^*_{8,10} \quad s_{7,10} = s_{8,10} = 0$$

  (ii) For node 4, the time-slot region length is $T - \mathbf{a}$.

$$T - \mathbf{a} = s_{4,8} + s_{4,9} + s_{4,10}$$

  By letting $s^{**}_{i,j}$ be its solution, a final natural number solution is:

$$s_{4,8} = s^{**}_{4,8}, \quad s_{4,9} = s^{**}_{4,9}, \quad s_{4,10} = s^{**}_{4,10}$$

Pattern 2 as illustrated in Fig. 5 is adopted when node group S_Z is a bottleneck. We solve a sub-problem for group S_Z first. In group S_X, $s_{2,2}$ and $s'_{2,1}$ cannot be 0 at the same time, in any optimal schedule.

$$M_1 = (1 - q_1^{s_{1,1}+s'_{1,1}}),$$
$$M_2 = \begin{cases} (1 - q_1^{s'_{2,1}+s_{2,1}})(1 - q_2^{s'_{2,2}}) & \text{if} \quad s_{2,2} = 0, \\ (1 - q_1^{s_{2,1}})(1 - q_2^{s'_{2,2}+s_{2,2}}) & \text{if} \quad s'_{2,1} = 0, \end{cases}$$
$$M_3 = (1 - q_1^{s_{3,1}})(1 - q_2^{s_{3,2}})(1 - q_3^{s_{3,3}})$$

In group S_Y,

$$M_5 = (1 - q_6^{s_{5,6}})(1 - q_7^{s_{5,7}})$$

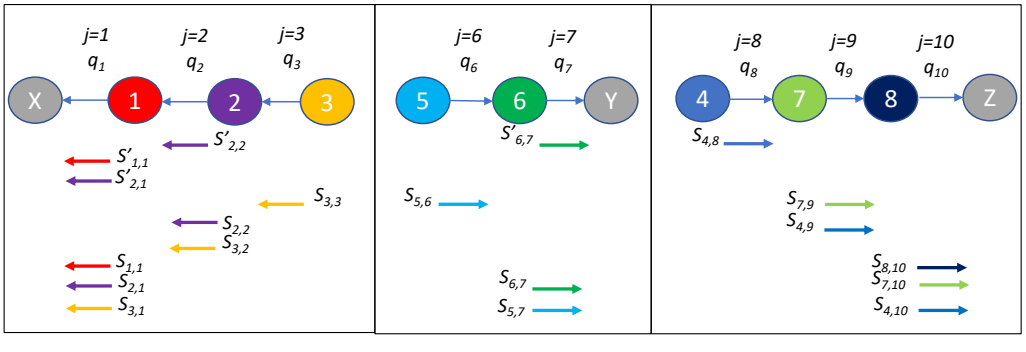

Figure 5: Transmission scheduling on 3-2-3 model (pattern 2, all r_i=1)

$$M_6 = (1 - q_7^{s_{6,7}+s'_{6,7}})$$

In group S_Z,

$$M_4 = (1 - q_8^{s_{4,8}})(1 - q_9^{s_{4,9}})(1 - q_{10}^{s_{4,10}})$$
$$M_7 = (1 - q_9^{s_{7,9}})(1 - q_{10}^{s_{7,10}})$$
$$M_8 = (1 - q_{10}^{s_{8,10}})$$

The following process is almost the same approach as Pattern 1. To get a slot allocation in group S_Z that maximizes $M_4 M_7 M_8$ subject to

$$T = s_{8,10} + s_{7,9} + s_{7,10} + s_{4,8} + s_{4,9} + s_{4,10},$$

we have

$$s_{4,10} = s_{7,10} = s_{8,10} = -\frac{\log(1 - \gamma \log(q_{10}))}{\log(q_{10})}$$
$$s_{4,9} = s_{7,9} = -\frac{\log(1 - \gamma \log(q_9))}{\log(q_9)}, \quad s_{4,8} = -\frac{\log(1 - \gamma \log(q_8))}{\log(q_8)}$$

where γ can be numerically solved to get the real number solution of the relaxed problem, and then obtain the natural number solution $\{s^*_{i,j}\}$ for S_Z.

Next, the obtained solution $s^*_{4,8}$ for S_Z is used to solve group S_Y. Starting from the tentative maximization of $M_5 M_6$ without considering $s'_{6,7}$ subject to

$$T = s_{5,6} + s_{5,7} + s_{6,7},$$

a final natural number solution $(s^*_{5,6}, s^*_{5,7}, s^*_{6,7}, (s'_{6,7})^*)$ is obtained after checking a few conditions (cases) for interference avoidance in S_Y with $s^*_{4,8}$ slots in S_Z in a similar manner as Pattern 1.

Finally, $s^*_{4,8}$ for is also used to solve group S_X. Starting from the tentative maximization of $M_1 M_2 M_3$ without considering $s'_{1,1}$, $s'_{2,1}$, $s'_{2,2}$ subject to

$$T = s_{1,1} + s_{2,1} + s_{2,2} + s_{3,1} + s_{3,2} + s_{3,3},$$

a final natural number solution $(s^*_{3,3}, s^*_{3,2}, s^*_{2,2}, (s'_{2,2})^*, s^*_{3,1}, s^*_{2,1}, s^*_{1,1}, (s'_{2,1})^*, (s_{1,1})^*)$ is obtained after checking a few case conditions for interference avoidance in S_X with $s^*_{4,8}$ slots in S_Z.

4.2. Static slot allocation for 2-2-4 model

Fig. 6 shows the 2-2-4 path model. In this example, since nodes 4 and 5 are assumed to be in the radio propagation distance, nodes 3 and 5 cannot send at the same time to avoid an interference at node 4. Similarly, since nodes 5 and 7 are in the propagation distance, nodes 4 and 5 cannot send at the same time to avoid an interference at node 7. On the other hand, 5 and 7 can send to their next node at the same time. We have two patterns for slot allocations. In Pattern 1, we prioritize the transmission in group S_Z (node 3-4-7-8) first, then group S_Y (node 5-6). In Pattern 2, we prioritize group S_Y first, then group S_Z. Note that group S_X is independent and solved separately.

Pattern 1 as illustrated in Fig. 7 is adopted when node group S_Z is a bottleneck. We solve a sub-problem for group S_Z first. In group S_X,

$$M_1 = (1 - q_1^{s_{1,1}}), \quad M_2 = (1 - q_1^{s_{2,1}})(1 - q_2^{s_{2,2}})$$

In group S_Z,

$$M_3 = (1 - q_4^{s_{3,4}})(1 - q_8^{s_{3,8}})(1 - q_9^{s_{3,9}})(1 - q_{10}^{s_{3,10}})$$
$$M_4 = (1 - q_8^{s_{4,8}})(1 - q_9^{s_{4,9}})(1 - q_{10}^{s_{4,10}})$$
$$M_7 = (1 - q_9^{s_{7,9}})(1 - q_{10}^{s_{7,10}}), \quad M_8 = (1 - q_{10}^{s'_{8,10}})$$

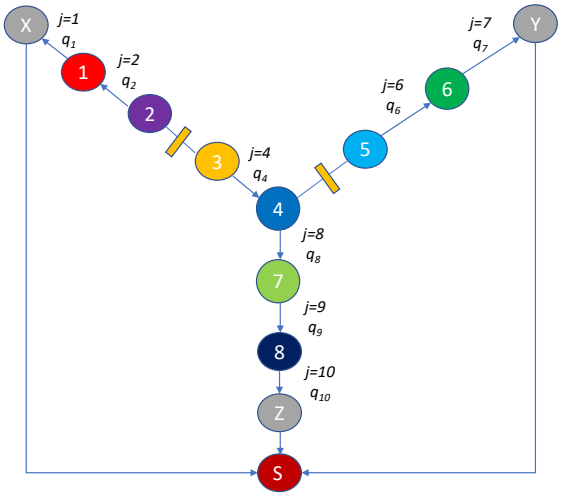

Figure 6: The 2-2-4 path model in the network topology

In group S_Y,

$$M_5 = (1-q_6^{s_{5,6}})(1-q_7^{s_{5,7}}), \quad M_6 = (1-q_7^{s_{6,7}+s'_{6,7}})$$

The process to get an optimal slot allocation is almost the same approach as the 3-2-3 model already explained. Therefore we only show group S_Z consisting of four nodes. To maximize $M_3M_4M_7M_8$ subject to

$$T = s_{3,4} + s_{3,8} + s_{4,8} + s_{3,9} + s_{4,9} + \cdots + s_{3,10},$$

we need to solve two equations independently

- Case 1: by ignoring $s_{3,4}$ (if $q_{10} \geq q_4$ in case that all $r_i = 1$),

$$T = 2s_{3,8} + 3s_{3,9} + 4s_{3,10}, \quad s'_{8,10} = s_{3,10}, \quad s_{3,4} = s'_{8,10} \tag{9}$$

- Case 2: by ignoring $s_{8,10}$ (if $q_{10} < q_4$ in case that all $r_i = 1$),

$$T = s_{3,4} + 2s_{3,8} + 3s_{3,9} + 3s_{3,10}, \quad s'_{8,10} = s_{3,4} \tag{10}$$

By solving Eq. (9) and Eq. (10) and selecting the best one, a natural number solution for S_Z is finally obtained. Based on that, $s^*_{3,4} + 2s^*_{3,8}$ is used to solve group S_Y.

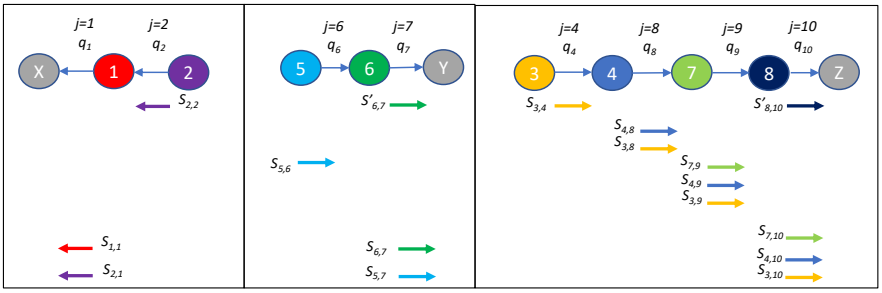

Figure 7: Transmission scheduling on the 2-2-4 model (pattern 1, all r_i=1)

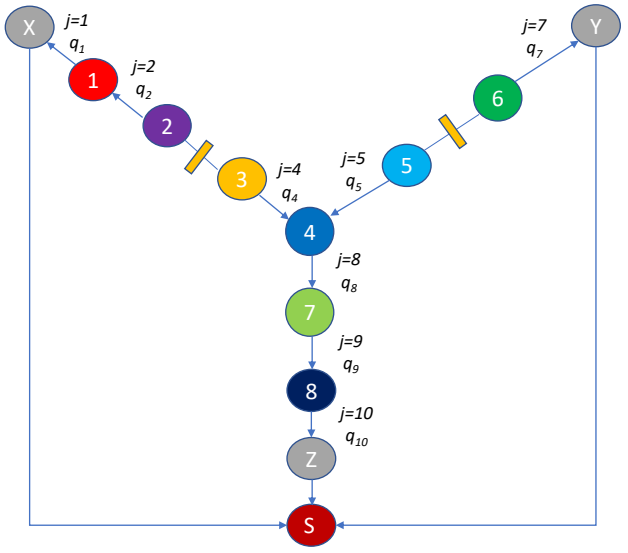

Figure 8: The 2-1-5 path model in the network topology

4.3. Static slot allocation for 2-1-5 model

Fig. 8 shows the 2-1-5 path model. In this example, since nodes 3, 4, and 5 are assumed to be in the radio propagation distance, nodes 3, 4 and 5 cannot send at the same time to avoid an interference. On the other hand, nodes 2 and 6 can send to their next node at the same time. Note that groups S_X and S_Y are independent and can be solved separately. Therefore, we need only a single pattern as illustrated in Fig. 9.

In group S_X,

$$M_1 = (1-q_1^{s_{1,1}}), \quad M_2 = (1-q_1^{s_{2,1}})(1-q_2^{s_{2,2}})$$

In group S_Z,

$$M_3 = (1-q_4^{s_{3,4}})(1-q_8^{s_{3,8}})(1-q_9^{s_{3,9}})(1-q_{10}^{s_{3,10}})$$
$$M_5 = (1-q_5^{s_{5,5}})(1-q_8^{s_{5,8}})(1-q_9^{s_{5,9}})(1-q_{10}^{s_{5,10}})$$

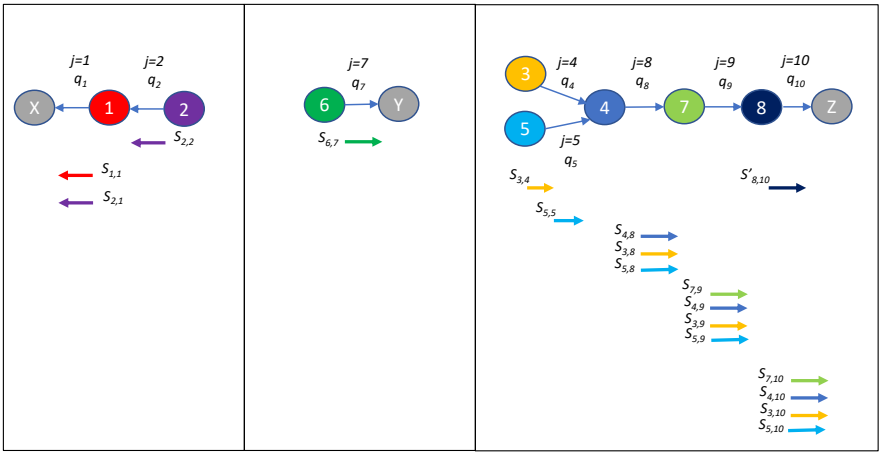

Figure 9: Transmission scheduling on 2-1-5 model (all r_i=1)

$$M_4 = (1-q_8^{s_{4,8}})(1-q_9^{s_{4,9}})(1-q_{10}^{s_{4,10}})$$

$$M_7 = (1-q_9^{s_{7,9}})(1-q_{10}^{s_{7,10}}), \quad M_8 = (1-q_{10}^{s_{8,10}+s'_{8,10}})$$

In group S_Y,

$$M_6 = (1-q_7^{s_{6,7}})$$

The process to get an optimal slot allocation is almost the same approach as the previous models. We only mention group S_Z. To maximize $M_3M_5M_4M_7M_8$ subject to

$$T = s_{3,4} + s_{5,5} + s_{3,8} + s_{4,8} + s_{3,9} + \cdots + s_{3,10},$$

two cases should be examined and select the best one. One case is to ignore $s_{8,10}$, (i.e., node 8 does not generate its packet), and the other case is to ignore $s_{3,4}$ and $s_{5,5}$, (i.e., nodes 3 and 5 do not generate their packets; instead, node 4 generates three packets).

5. Numerical results

On our example of the Y-shaped network topology, we show a few numerical results for three different path models to evaluate the performance of derived time-slot allocations in four different cases in terms of the setting of link loss rates $\{q_{i,j}\}$ shown in Table 1; packet generation rates are uniform ($r_i = 1$) and the total number T of time-slots is $T = 20$ or $T = 30$. Highly lossy links (links with high loss rates) are located near gateway Y in Case 1; near gateway X in Case 2; near gateways X and Y in Case 3 and at link 2 towards gateway X in Case 4. Matlab is used to get the solutions of the maximization problems for the path model in the way described in Section 4. As a performance metric, the Theoretical Upper-Bound (TUB) value and the Model-based Computed (COM) value are used. TUB is the theoretical maximum value of the objective function M(s) in the relaxed version of the maximization problem (i.e., any real number can be used). COM is the computed probability of delivering all packets using an optimal slot allocation according to a natural number solution of the original integer-constraint maximization problem.

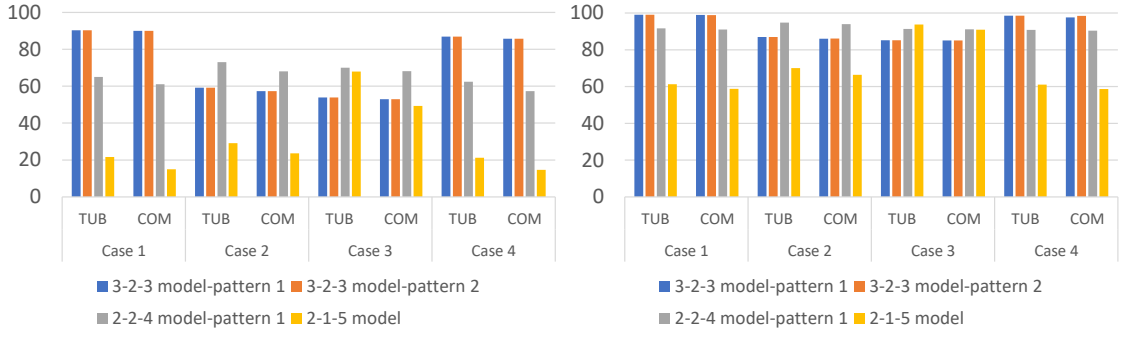

Figure 10: Probability of successful delivery for all nodes with T=20 (left) and T=30 (right)

First, we explain the main results in Fig. 10. The TUB value is not lower than the COM value in general simply because the TUB value is the theoretical maximum value of the objective function. However, the actual performance, the success delivery probability for all packets, is represented by the COM value not the TUB value. At least in four cases of packet loss rate setting (Cases 1, 2, 3, and 4) and two cases of the total number of slots ($T = 20, 30$), both patterns of the 3-2-3 model can achieve the almost equal performance regardless of whether group S_X or S_Z is prioritized. It is attributed to the balanced locations of the separated links, which is investigated later. In Case 1 and Case 4, the 3-2-3 model illustrates a significantly higher performance than its counterparts. In addition, in case of $T = 30$, the 3-2-3 model shows more than 80 percent of the successful delivery in all cases. Noticeably, the high resilience of this model possibly stems from the relatively equal number of nodes in all groups. On the other hand, in Case 2, Pattern 1 in the 2-2-4 model has been demonstrated to be more effective where there are three successive high loss links (1,2, and 3) from gateway X. Since link 3 is included in group S_X of the 3-2-3 model, its high packet loss

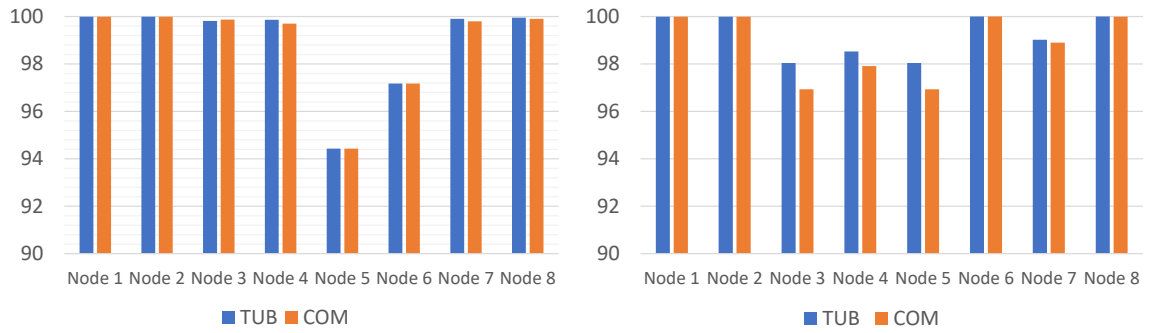

Figure 11: Probability of successful delivery for each node with $T = 30$ in Case 3, Pattern 1 in the 2-2-4 model (left), the 2-1-5 model (right)

Table 1
Packet loss rate on each link

Case	q_1	q_2	q_3	q_4	q_5	q_6	q_7	q_8	q_9	q_{10}
1	0.3	0.1	0.3	0.3	0.2	0.5	0.3	0.2	0.3	0.2
2	0.5	0.4	0.5	0.3	0.2	0.3	0.2	0.2	0.3	0.1
3	0.4	0.3	0.6	0.1	0.1	0.7	0.7	0.1	0.1	0.1
4	0.1	0.5	0.1	0.3	0.2	0.3	0.5	0.2	0.2	0.3

rate adversely affects the performance of the 3-2-3 model. In contrast, link 3 is a separation link of the 2-2-4 model and thus does not affect the 2-2-4 model at all. Note that, in case of a less number of totally available slots ($T = 20$) in Fig. 10, although the probability of successful delivery reduces significantly in all 4 cases, the overall characteristics are almost unchanged.

Next, we focus on Case 3 and compare the 2-2-4 model (Pattern 1) and the 2-1-5 model. The 2-1-5 model includes 5 nodes in group S_Z and generally suffers from the accumulated number of packets to be transmitted with the accumulated loss rates on links in the transmitting process toward gateway Z. However, in Case 3, the 2-1-5 model is the best model among all models with patterns in terms of TUB, while Pattern 1 in the 2-2-4 model is best in terms of COM. Case 3 has three bad links 3, 6,and 7 with extremely high loss rates 0.6, 0.7, and 0.7, respectively. Therefore, the 2-2-4 model in which link 3 is a separation link and the 2-1-5 model in which links 3 and 6 are separation links outperform the 3-2-3 model in which none of those three bad links is a separation link. Fig. 11 shows the probability of successful delivery for each node (for a packet generated by the node) in Case 3 with Pattern 1 in the 2-2-4 model and with the 2-1-5 model. For the 2-2-4 model in the left of Fig. 11, since nodes 5 and 6 in group S_Y rely on two bad links 6 and 7, the success probabilities for those two nodes are considerably lower than other nodes. However, the gap between TUB and COM values is negligible. For the 2-1-5 model in the right of Fig. 11, since group S_Y consists only of a single node (6), an enough number of slots can mitigate the impact of the bad link 7 and thus the performance in S_Y is not degraded. On the other hand, the performance in group S_Z (i.e., for nodes 3, 5, 4, 7, and 8) is degraded because the number of nodes in the group is larger. Moreover, the gap between TUB and COM values on those nodes is not negligible. Therefore, due to the degradation of the COM performance in S_Z in the model 2-1-5, those two models show the almost same COM performance. This gap can be explained by a less number of slots allocated to a packet in S_Z in the 2-1-5 model (see Fig. 9 in Section 4). When a more number of nodes and links in a group are scheduled with a less number of totally available slots, the number of slots allocated to each packet on each link is also less, and thus the performance impact of decreasing one slot becomes larger.

Then, we investigate the difference between two patterns in the model 3-2-3 in Case 1. Table 2 and Table 3 show slot allocations for Pattern 1 and Pattern 2 in the 3-2-3 model with $T = 30$. On Pattern 1, in groups S_X and S_Y respectively, the most upstream nodes 3 and 5 send packets first at the beginning of one cycle period. Hence, in group S_Z, the downstream nodes 7 and 8 send packets at that moment instead of the most upstream node 4. This involves a separation of allocated slots for nodes 7 and 8 (i.e., links 9 and 10) into two different times such as $(s'_{7,10}, s_{7,10})$. In contrast, on Pattern 2, the most upstream node 4 in S_Z sends packets first at the beginning of one cycle period,

Table 2
Slot allocations for Pattern 1 in the 3-2-3 model with T=30 (case 1)

	$s_{1,1}$	$s'_{1,1}$	$s_{2,1}$	$s'_{2,1}$	$s_{2,2}$	$s'_{2,2}$	$s_{3,1}$	$s_{3,2}$	$s_{3,3}$	$s_{4,8}$	$s_{4,9}$	$s_{4,10}$
TUB	5.83	0	5.83	0	3.33	0	5.83	3.33	5.83	4.57	5.68	4.57
COM	6	0	6	0	3	0	6	3	6	4	6	5
	$s_{5,6}$	$s_{5,7}$	$s_{6,7}$	$s'_{6,7}$	$s_{7,9}$	$s'_{7,9}$	$s_{7,10}$	$s'_{7,10}$	$s_{8,10}$	$s'_{8,10}$		
TUB	13.52	8.24	8.24	0	0	5.86	1.48	3.09	0	4.57		
COM	14	8	8	0	0	6	1	3	0	5		

Table 3
Slot allocations for Pattern 2 in the 3-2-3 model with T=30 (case 1)

	$s_{1,1}$	$s'_{1,1}$	$s_{2,1}$	$s'_{2,1}$	$s_{2,2}$	$s'_{2,2}$	$s_{3,1}$	$s_{3,2}$	$s_{3,3}$	$s_{4,8}$	$s_{4,9}$	$s_{4,10}$
TUB	1.27	4.57	5.83	0	3.33	0	5.83	3.33	5.83	4.57	5.86	4.57
COM	1	4	6	0	3	0	6	4	6	5	6	5
	$s_{5,6}$	$s_{5,7}$	$s_{6,7}$	$s'_{6,7}$	$s_{7,9}$	$s'_{7,9}$	$s_{7,10}$	$s'_{7,10}$	$s_{8,10}$	$s'_{8,10}$		
TUB	13.52	8.24	3.67	4.57	5.86	0	4.57	0	4.57	0		
COM	13	8	4	5	6	0	4	0	4	0		

and thus the downstream nodes 1, 2 (in S_X) and 6 (in S_Y) send packets at that moment instead of the most upstream nodes. This also involves a separation of allocated slots for nodes 1, 2, and 8 (i.e., links 2, 3, and 7) into two different times such as $(s'_{1,1}, s_{1,1})$ and $(s'_{6,7}, s_{6,7})$. Although the slot allocation patterns are different, the TUB performance is unchanged between two patterns as shown in Fig. 10. This can be explained as follows. By comparing the TUB case in Table 2 and Table 3, we can see that $s_{1,1}$ and $s_{6,7}$ in Pattern 1 are almost equal to $s'_{1,1} + s_{1,1}$ and $s'_{6,7} + s_{6,7}$ in Pattern 2, respectively. Oppositely, $s'_{7,10} + s_{7,10}$ in Pattern 1 is equal to $s_{7,10}$ in Pattern 2. Since $s_{1,1}$ and $s'_{1,1} + s_{1,1}$ have the same impact on the performance, the TUB performances of Pattern 1 and Pattern 2 are the same. On the other hand, due to an unavoidable gap between a real number value of $s_{i,j}$ in TUB case and a natural number value of $s_{i,j}$ in COM, there may be a small difference in the COM performances of Pattern 1 and Pattern 2. For example, $s_{1,1}$ in Pattern 1 is 6 in COM but $s'_{1,1} + s_{1,1}$ in Pattern 2 is equal to $4 + 1 = 5$ in COM as well.

Finally we compare the performance of the proposed method (Pattern 1 of the 3-2-3 model) to that of a conventional approach based on an existing work, although the original targeted scenario is different from us. We consider Ergen's method [10] as a well-known typical existing work and apply it to 3-2-3 path model with link loss conditions in Case 1 and Case 4. Ergen's method assumes a tree topology with a single sink node (a gateway in our setting) and aims to find a smallest length interference-free allocation of slots during which the packets generated at each node reach the sink; retransmissions due to packet loss are not considered. Therefore, how to apply Ergen's method is not trivial and explained in Appendix B; we call it the Ergen-based method.

Fig. 12 demonstrates the advantage of the proposed method (Pattern 1) to the Ergen-based method in our scenarios in terms of the probability that all packets are successfully delivered to one of the gateways with redundant transmissions within one cycle period. It is not surprising because the proposed method (Pattern 1) has been designed to optimize the number of redundant transmissions of the same packet on each link by considering the restriction of the total number of slots in one cycle period and the packet loss rates of links. For example, for packet transmissions to gateway X in Case 4, the packet loss rates of links 1, 2, and 3 are 0.1, 0.5, and 0.1, respectively. In this case with the total number $T = 30$ of slots, the proposed method (pattern 1) derives the optimal numbers of redundant transmissions of a packet on links 1, 2, and 3, they are 3, 9, and 3, respectively. On the other hand, since the Ergen-based method derives a smallest length interference-free allocation of slots, that pattern is just repeated within one cycle period and thus the numbers of redundant transmissions of a packet on each link is identically 5.

When comparing Case 1 and Case 4, although the average packet loss rate over the links used in transmission is unchanged, the performance of the Ergen-based method decreases significantly in Case 4. The difference between two cases for the Ergen-based method is caused by the locations of highly lossy links. For example, for packet transmissions to gateway X in Case 1, links 1 and 3 are lossy and the packets generated only at node 3 (the most upstream node) suffer from packet losses on both two links as shown in Fig. 13 (left). On the other hand, in Case 4, link 2 is highly lossy and the packets generated both at nodes 2 and 3 as shown in Fig. 13 (right). In contrast, such a degradation in

Case 4 is not seen in the proposed method. This is because the proposed method (Pattern 1) appropriately distributes the totally available slots over all links to maximize the probability that all packets are successfully delivered within one cycle period.

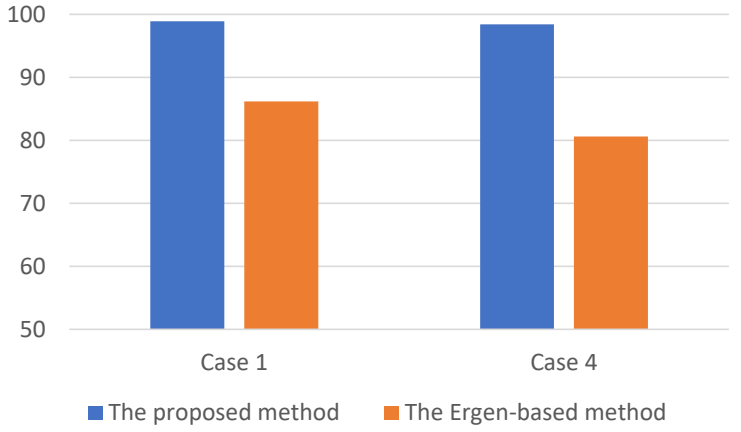

Figure 12: Probability of successful delivery for all nodes with T=30 (Blue): the proposed method , (Orange): the Ergen-based method, (Left): Case 1, (Right): Case 4

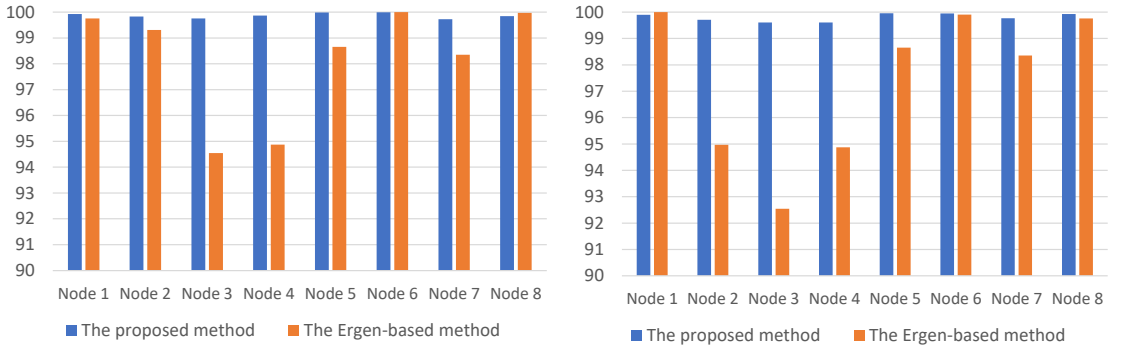

Figure 13: Probability of successful delivery for each node with T=30 (Blue): the proposed method, (Orange): the Ergen-based method; (Left): Case 1, (Right): Case 4

6. Discussion

We address a few issues that are not well mentioned in the main part of this paper but necessary to implement and extend our proposed scheme into practical systems.

Firstly, our scheme is applicable to heterogeneous packet generation rates of nodes and heterogeneous data transmission rates of links, although only homogeneous cases were explained in this paper for concise formulations. In reality, each node may support different numbers of and/or types of sensors, and thus the number of packets necessary to convey them in one cycle period may differ. In addition, different types of backbone links may be mixed in the same network with the different data transmission rate to adjust some restrictions, e.g., physical distance and cost. In our preliminary work on the tandemly-arranged topology networks with two gateways, we have shown the formulations and results on heterogeneous packet generation rates [4] and data transmission rates [3]. How the different packet generation rates (r_i for node i) can be managed in our setting of Y-shaped topology is shown in Appendix A. Furthermore, the number of nodes can be extended, although only 8-node example was shown. In general, even if the number of nodes, i.e., the length of a path, is increased, the interference patterns around the central node are unchanged. Only the

chances of a concurrent use of the same time-slots for the same direction transmissions by two distanced nodes in the path is increased. However, an investigation on performance impacts and implications to scheduling design remains as future work.

Secondly, in this paper, our scheme only adopts a basic redundant transmission scheme in which a node just redundantly transmits each of its possessed packets in a specific times according to the given time-slot allocation. However it is well-known that a packet-level coding as FEC increases the success probability of packet delivery, although it introduces the encoding/decoding overhead into the system. Each node can combine multiple different packets its possessed by using some coding scheme and transmits possibly different coded packets within the allocated slots; those coded packets are decoded in the final receiver, e.g., a central data collection server. Our previous work [3] have shown the benefits of XOR-based simple coding with consideration of fairness among nodes. A detailed design and performance investigation of packet-coding in Y-shaped topology setting remain as future work.

Finally, our scheme is on a centrally-managed transmission scheduling for a network of relay nodes with gateways, and implicitly assumes a central management server that compute a global time-slot allocation. Therefore, the next research will concentrate on the system architecture for real implementation. More specifically, a scheme to exchange and share the involved information is necessary (i) for a server to know or estimate a network topology and related information such as data transmission rates (bandwidths) of links, distances between nodes, packet loss rates on links, and packet generation rates at nodes; and (ii) for each node to know a derived transmission schedule. In particular, the information exchange of (ii) requires an opposite direction communication from gateways to each node and is needed not only at the initial phase of the system but every time when environmental conditions change or periodically with a relatively long time interval.

7. Concluding remarks

In this paper, we focus on a wireless sensor network of Y-shaped topology (a linear topology with three gateways at the edges), and pose the problem to find a static interference-free allocation of time-slots to maximize the theoretical probability that all packets are successfully delivered through lossy links to one of the gateways with redundant transmissions within a given one cycle period. We have proposed a general framework to derive such a time-slot allocation on any type of Y-shaped topology, in which an optimal number of slots for each packet on each link is obtained by solving a relaxed version of the problem to maximize the objective function subject to the total number of slots in one cycle period. Our work presented three types of the path models on Y-shaped topology. We showed a detail formulation on each path model for the optimization to the packet scheduling . All models were evaluated in different cases to select the appropriate one for each case.

Acknowledgements

The research results have been achieved by the "Resilient Edge Cloud Designed Network (19304)," NICT, and by JSPS KAKENHI JP20K11770, Japan.

Appendix A

We explain how to derive Eq.(5). For group S_X in transmission pattern 1 of the 3-2-3 model, let M_i be the theoretical probability that a single packet generated by node i is successfully delivered to gateway X with the basic redundant transmission scheme. According to Fig. 4, we have

$$M_1 \;=\; (1-q_1^{s_{1,1}}),\;\; M_2 \;=\; (1-q_1^{s_{2,1}})(1-q_2^{s_{2,2}}),\;\; M_3 \;=\; (1-q_1^{s_{3,1}})(1-q_2^{s_{3,2}})(1-q_3^{s_{3,3}}),$$

by letting $s_{i,j}$ be the number of allocated slots for one packet generated by node i on link j.

Our final goal is to find a slot allocation maximizing the theoretical probability M that all packets in one cycle period are successfully delivered to gateway X with the basic redundant transmission scheme. The exact formulation of M is somewhat complicated. By letting $s_{i,j,k}$ be the number of allocated slots for the k-th packet generated by node i on link j, this probability M is

$$\prod_{j=1}^{r_1}(1-q_1^{s_{1,1,j}})\prod_{j=1}^{r_2}(1-q_1^{s_{2,1,j}})(1-q_2^{s_{2,2,j}})\prod_{j=1}^{r_3}(1-q_1^{s_{3,1,j}})(1-q_2^{s_{3,2,j}})(1-q_3^{s_{3,3,j}}).$$

However, since we deal with a relaxation version of the maximization problem to apply the Lagrangian multiplier method, the formulation of M can be simpler in the relaxation version by considering $s_{i,j,k} = s_{i,j}$ for $\forall k$:

$$M = M(\mathbf{s}) = M_1^{r_1} M_2^{r_2} M_3^{r_3} \tag{11}$$

where $\mathbf{s} = (s_{1,1}, s_{2,1}, s_{3,1}, s_{2,2}, s_{2,3}, s_{3,3})$ and $s_{i,j} (> 0)$ are not restricted to natural numbers.

Please note that "$s_{i,j,1} \neq s_{i,j,2}$" may happen in the original maximization problem for slot allocation due to the total slot number is restricted by a given T. Therefore, as we showed in Section 4, we should find the exact optimal natural numbers $\{s_{i,j,k} | k = 1, 2, \ldots, r_i\}$ after obtaining a real number solution $\{s_{i,j}\}$.

The relaxation version problem can be solved as follows.

$$\max\ M \ \text{ subject to } \ T = r_1 s_{1,1} + r_2(s_{2,1} + s_{2,2}) + r_3(s_{3,1} + s_{3,2} + s_{3,3})$$

where M is defined in Eq.(11).

The corresponding Lagrangian function is:

$$L \ = \ M - \lambda(r_1 s_{1,1} + r_2(s_{2,1} + s_{2,2}) + r_3(s_{3,1} + s_{3,2} + s_{3,3}) - T).$$

First we define two notations for conciseness.

$$G(q, x) \ = \ \frac{-q^x \log q}{1 - q^x}, \ \ F(q, y) \ = \ -\frac{\log(1 - y \log q)}{\log q} \tag{12}$$

where $G(q, x) = \dfrac{1}{y} \ \Leftrightarrow \ x = F(q, y)$.

If $\mathbf{s}$ is a soluition within the internal region, $\dfrac{\partial L}{\partial s_{i,j}} = 0$ should be held for every (i, j). Hence, by differentiating L with respect to $s_{1,1}$, we have

$$\begin{aligned}
\frac{\partial M}{\partial s_{1,1}} \ &= \ \frac{\partial M_1}{\partial s_{1,1}} (r_1 M_1^{r_1 - 1}) M_2^{r_2} M_3^{r_3} \\
&= \ r_1(-q_1^{s_{1,1}} \log q_1) M_1^{r_1 - 1} M_2^{r_2} M_3^{r_3} = r_1 G(q_1, s_{1,1}) M, \\
\frac{\partial L}{\partial s_{1,1}} \ &= \ r_1 G(q_1, s_{1,1}) M - r_1 \lambda \ = \ 0, \\
G(q_1, s_{1,1}) \ &= \ \frac{\lambda}{M}
\end{aligned} \tag{13}$$

where G is defined in Eq.(12).

In the same way, we have:

$$\frac{\partial L}{\partial s_{i,j}} \ = \ r_i G(q_j, s_{i,j}) M - r_i \lambda \ = \ 0,$$

and thus,

$$G(q_1, s_{2,1}) = G(q_1, s_{3,1}) = G(q_2, s_{2,2}) = G(q_2, s_{3,2}) = G(q_3, s_{3,3}) \ = \ \frac{\lambda}{M} \tag{14}$$

From Eqs.(13) and (14), by letting $\alpha = \dfrac{M}{\lambda}$ as an adjunct variable, we have an explicit expression of each $s_{i,j}$ with an unknown positive variable α:

$$s_{1,1} = s_{2,1} = s_{3,1} = F(q_1, \alpha), \ \ s_{2,2} = s_{3,2} = F(q_2, \alpha), \ \ s_{3,3} = F(q_3, \alpha) \tag{15}$$

where F is defined in Eq.(12).

Appendix B

Ergen's work [10] is well-known and provide a centrally-managed TDMA scheduling method for wireless sensor networks. In the work, general tree topologies with a single sink node (a gateway in our setting) are targeted, and the goal is to find a static interference-free allocation of time-slots so as to minimize the number of slots during which all packets generated at nodes reach the gateway through loss-free links; packet retransmissions against packet loss are not considered. On the other hand, in our targeting scenarios with Y-shaped topology, gateways are located at the edges and all links are lossy. Furthermore, our goal is to find a static interference-free allocation of time-slots by considering packet retransmissions so as to maximize the theoretical probability that all packets generated at nodes successfully reach one of the gateways through loss links within the total number T of slots. Therefore, how to apply Ergen's method to our scenarios is not trivial.

Ergen's method consists of two steps. The first is to color the conflict-graph that represents the potential interferences; the nodes assigned the same color can transmit a packets at the same slot. The second is, based on the obtained coloring, to schedule the packet transmissions at nodes by allocating slots to each node (i.e., each link) so that the length of interference-free allocation of slots is minimized during which all packets reach the gateway; each node transmits a packet to the next node on an allocated slot towards a gateway. Note that the coloring is not an easy task in general and there are a number of heuristics proposed; but it is easy in our scenarios thanks to the linear feature of Y-shaped topology. Furthermore, there are originally the node-based and the level-based ones in Ergen's method; but they are essentially the same in our scenarios. In scheduling, the active node is defined as a node who currently has at least one packet to transmit; the superslot is defined as a collection of consecutive slots such that each active node at the beginning of the superslot transmits at least one packet during the superslot. An algorithm constructs a superslot to move one packet from each active node to its neighbor and repeats this process until all packets reach the gateway.

Hereinafter, we explain the Ergen-based method, that is a simple application of Ergen's method to the Y-shaped model with link loss conditions, on the 3-2-3 path model example shown in Fig. 3. First, in response to three gateways, there are three groups S_X (node 3-2-1), S_Y (node 5-6), and group S_Z (node 4-7-8). On coloring, not only among successive nodes in each group, but also the interferences at the tail among three groups should be considered. That is, nodes 3 and 4 cannot send packets simultaneously (to avoid interference at node 7) because nodes 3 and 7 are assumed in the radio propagation distance. The same problem exists in the transmission of nodes 5 and 4. However, nodes 3, 5, and 7 can send packets to their next node simultaneously. Fig. 14 shows an example color assignment in the Ergen-based method.

In the same manner as the proposed method in Section 4.1 for the 3-2-3 model, we consider two patterns for slot allocations. In Pattern 1, we prioritize the transmission in groups S_X (node 3-2-1) and S_Y (node 5-6) first, and continue with group S_Z (node 4-7-8). In Pattern 2, we prioritize the transmission group S_Z first. Based on the coloring in Fig. 14, we explain Pattern 1 scheduling in Fig. 15. The slot allocation starts from group S_X and node 3 in S_X. In the first superslot, since each node of three nodes has its own packet and is colored differently, slot 1, slot 2, and slot 3 are assigned to node 3, node 2, and node 1, respectively. Then, since node 3 has no packet, the next superslot consists of slot 4 and slot 5 for node 2 and node 1, respectively. At slot 6, only node 1 has a packet to transmit, that is the third superslot. Hence all three packets can reach the gateway X through loss-free links over three superslots with six slots in total; this number of slots is minimum. This slot allocation process is executed similarly in group S_Y and then in S_Z. In group S_Y, node 5 is first; in group S_Z, node 4 first. Then a redundant transmission scheme is introduced against packet loss by simply repeating the same allocation pattern of slots in each group. In this example, S_X, S_Y, and S_Z require 6 slots, 3 slots, and 6 slots for all packets in each group to reach gateways X, Y, and Z, respectively. Therefore, with the total number $T = 30$ of slots, those slot allocation patterns can be repeated by 5 times, 10 times, and 5 times in S_X, S_Y, and S_Z, respectively. The resulting overall allocation is shown in in Fig. 15.

The slot allocations in Pattern 1 and Pattern 2 by the Ergen-based method are shown in Fig. 16. Note that the targeted performance, the probability that all packets generated at nodes successfully reach one of the gateways within the total number $T = 30$ of slots, is unchanged in both patterns. The performance is computed as follows. Let $M_i^{(E)}$ be the theoretical probability that a single packet generated by node i is successfully delivered to gateway X, gateway Y or gateway Z in the Ergen-based method with the above mentioned redundant transmission scheme in case of $T = 30$. For example, the probability that the packet generated by node 1 does not reach gateway X through link 1 during a single pattern is equal to the packet loss rate q_1 on link 1, and this pattern is repeated by 5 times. Hence, $M_1^{(E)}$ is $1 - q_1^5$.

In group S_X

$$M_1^{(E)} = 1 - q_1^5,$$

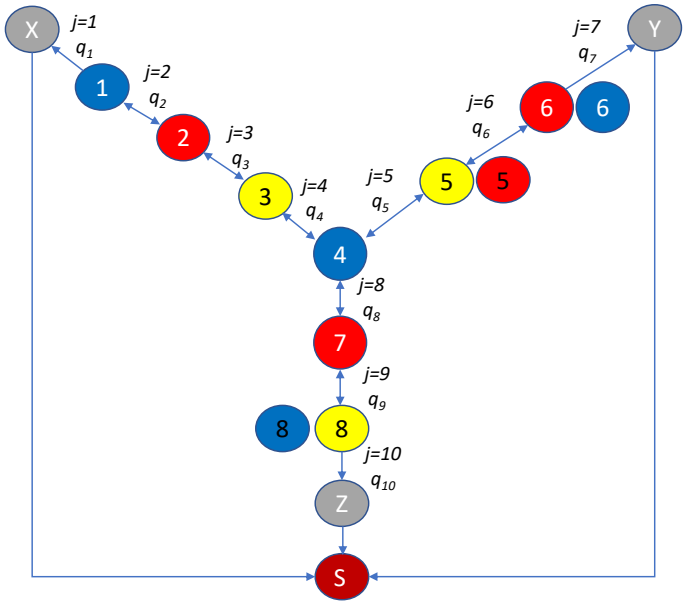

Figure 14: Assignment of colors to the 3-2-3 model using the Ergen-based method

Group X

Superslot	1			2		3	4			5		6	7			8		9	10			11		12	13			14		15
Slot	1	2	3	4	5	6	7	8	9	10	11	12	13	14	15	16	17	18	19	20	21	22	23	24	25	26	27	28	29	30
Color																														
Schedule	S3	S2	S1	S2	S1	S1	S3	S2	S1	S2	S1	S1	S3	S2	S1	S2	S1	S1	S3	S2	S1	S2	S1	S1	S3	S2	S1	S2	S1	S1

Group Z

Superslot	1			2		3	4			5		6	7			8		9	10			11		12	13			14		15
Slot	1	2	3	4	5	6	7	8	9	10	11	12	13	14	15	16	17	18	19	20	21	22	23	24	25	26	27	28	29	30
Color																														
Schedule	S8	S7	S4	S7	S8	S8	S8	S7	S4	S7	S8	S8	S8	S7	S4	S7	S8	S8	S8	S7	S4	S7	S8	S8	S8	S7	S4	S7	S8	S8

Group Y

Superslot	1		2		3	4		5		6	7		8		9	10		11	12		13	14		15		16	17		18	19		20
Slot	1	2	3	4	5	6	7	8	9	10	11	12	13	14	15	16	17	18	19	20	21	22	23	24	25	26	27	28	29	30
Color																														
Schedule	S5	S6	S6	S5	S6	S6	S5	S6	S6	S5	S6	S6	S5	S6	S6	S5	S6	S6	S5	S6	S6	S5	S6	S6	S5	S6	S6	S5	S6	S6

Figure 15: Transmission scheduling and assignment of colors using the Ergen-based method

$$M_2^{(E)} = 1-(1-(1-q_1)(1-q_2))^5,$$
$$M_3^{(E)} = 1-(1-(1-q_1)(1-q_2)(1-q_3))^5$$

In group S_Y

$$M_5^{(E)} = 1-(1-(1-q_6)(1-q_7))^5,$$
$$M_6^{(E)} = (1-q_7^5)$$

In group S_Z

$$M_4^{(E)} = 1-(1-(1-q_8)(1-q_9)(1-q_{10}))^5$$

$$
\begin{aligned}
M_7^{(E)} &= 1-(1-(1-q_9)(1-q_{10}))^5 \\
M_8^{(E)} &= (1-q_{10}^5),
\end{aligned}
$$

Let M_i be those probabilities by our proposed method, which are formulated in Eqs. (1), (2), and (3) in Section 4. The targeted performance by the Ergen-based method is $M^{(E)} = \prod_{i=1}^{8} M_i^{(E)}$, while that by the proposed method is $M = \prod_{i=1}^{8} M_i$. By comparing them, it can be proven that $M^{(E)}$ is not greater than M in general.

References

[1] D. P. A. I. Jawhar, N. Mohamed, Linear wireless sensor networks: Classification and applications, Journal of Network and Computer Applications 34 (2011) 1671–1682.

[2] M. T. Agussalim, Message transmission scheduling on tandem multi-hop lossy wireless links, Proc. the 14th IFIP International Conference on Wired/Wireless Internet Communications (WWIC2016) (2016) 28–39.

[3] M. T. R. Kimura, M. Shibata, Scheduling for tandemly-connected sensor networks with heterogeneous link transmission rates, Proceedings the 34th International Conference on Information Networking (ICOIN2020) (2020) 590–595.

[4] M. T. R. Yoshida, M. Shibata, Transmission scheduling for tandemly-connected sensor networks with heterogeneous packet generation rates, Proceedings the 12th International Conference on Intelligent Networking and Collaborative Systems (INCoS2020) 1263 (2020) 437–446.

[5] M. T. L.V. Nguyen, M. Shibata, Message transmission scheduling for multi-hop wireless sensor network with t-shaped topology, Proceedings of the 15-th International Conference on Broadband and Wireless Computing, Communication and Applications (BWCCA) 159 (2020) 120–130.

[6] D. D. V. D. D. A. Sgora, D. J. Vergados, A survey of tdma scheduling schemes in wireless multihop networks, ACM Computing Surveys 47 (2015) 1–39.

[7] V. N. P. L. Q. K. Jain, J. Padhye, Impact of interference on multi-hop wireless network performance, Proceedings of the 9th annual international conference on Mobile computing and networking 11 (2003) 66–80.

[8] S. Ramanathan, A unified framework and algorithm for channel assignment in wireless networks, Wireless Networks 5 (1999) 81–94.

[9] J. M. I. Rhee, A. Warrier, L. Xu, Drand: distributed randomized tdma scheduling for wireless ad-hoc network, IEEE Transactions on Mobile Computing 8 (2009) 1384–1396.

[10] P. V. S. C. Ergen, Tdma scheduling algorithms for wireless sensor networks, Wireless Networks 16 (2010) 985–997.

[11] T. U. F. I. M. Sasaki, T. Furuta, Tdma scheduling problem avoiding interference in multi-hop wireless sensor networks, Journal of Advanced Mechanical Design, Systems, and Manufacturing 10 (2016) JAMDSM0047.

[12] Y. D. B. Zeng, A collaboration-based distributed tdma scheduling algorithm for data collection in wireless sensor networks, Journal of Networks 9 (2014) 2319–2327.

[13] F. Ishizaki, Computational method using quantum annealing for tdma scheduling problem in wireless sensor networks, 13th International Conference on Signal Processing and Communication Systems (ICSPCS) (2019) (2019) 1–9.

[14] C. Buratti, R. Verdone, Joint scheduling and routing with power control for centralized wireless sensor networks, Wireless Networks 24 (2018) 1699–1714.

[15] G. H. H. N. H. Tokito, M. Sasabe, Load-balanced and interference-aware spanning tree construction algorithm for tdma-based wireless mesh networks, IEICE Transactions on Communications E93.B (2010) 99–110.

[16] K. K. P. Chaporkar, Throughput and fairness guarantees through maximal scheduling in wireless networks, IEEE TRANSACTIONS ON INFORMATION THEORY 54 (2008) 572–594.

Pattern 1

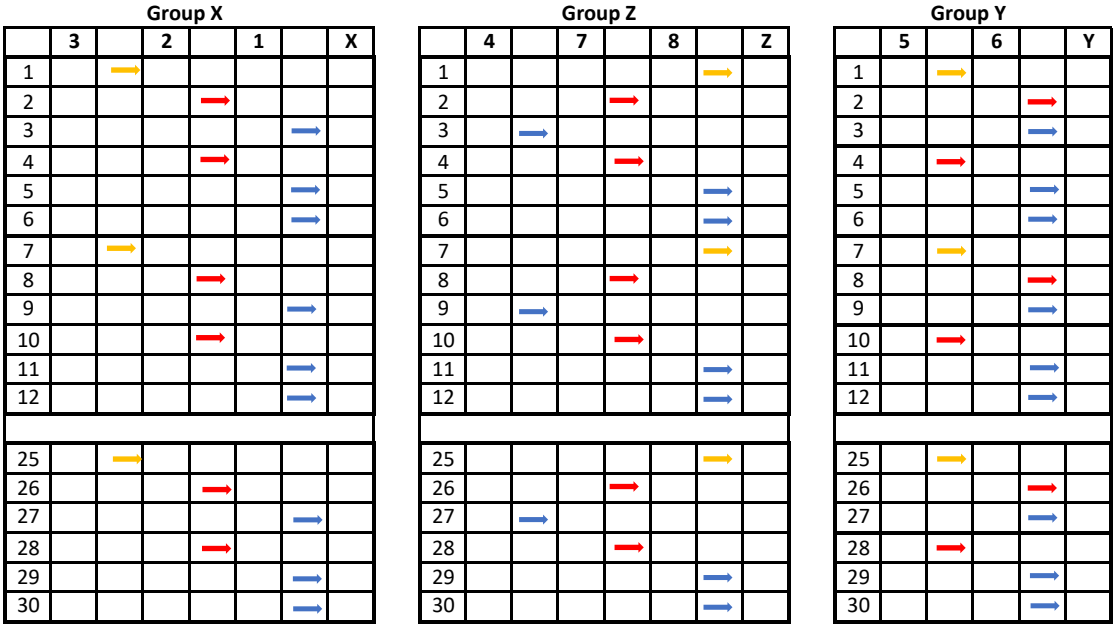

Pattern 2

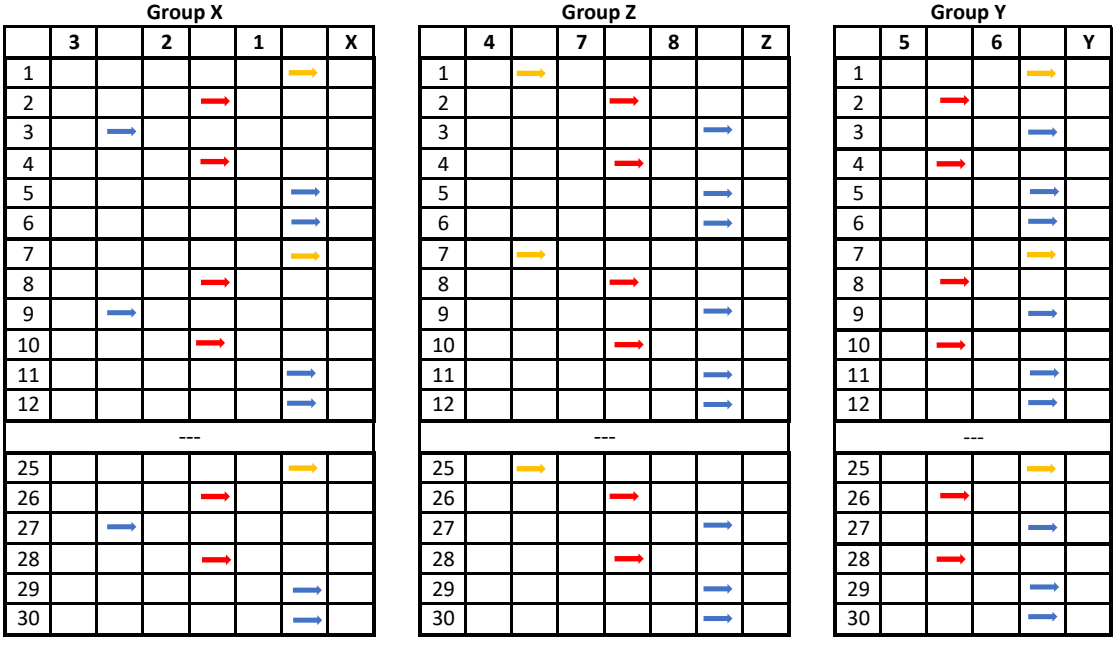

Figure 16: Detaited transmission scheduling of pattern 1 (up) and pattern 2 (down) using the Ergen-based method